Published in final edited form as:
Chem Res Toxicol. 2012 April 16; 25(4): 873–883. doi:10.1021/tx2004882.

Delivery method, target gene structure and growth properties of target cells impact mutagenic responses to reactive nitrogen and oxygen species

Min Young Kim[†,⊥], **Chang Hoon Lim**[‡], **Laura J. Trudel**[†], **William M. Deen**[‡], and **Gerald N. Wogan**[†,§,*]

[†]Biological Engineering Department, 77 Massachusetts Avenue, Cambridge, MA 02139

[‡]Chemical Engineering Department, 77 Massachusetts Avenue, Cambridge, MA 02139

[§]Chemistry Department, Massachusetts Institute of Technology, 77 Massachusetts Avenue, Cambridge, MA 02139

[⊥]College of Applied Life Sciences, Jeju National University, Jeju 690-756, Republic of Korea

Abstract

Dysregulated production of nitric oxide ($NO^{\bullet}$) and reactive oxygen species (ROS) by inflammatory cells *in vivo* may contribute to mutagenesis and carcinogenesis. Here we compare cytotoxicity and mutagenicity induced by $NO^{\bullet}$ and ROS in TK6 and AS52 cells, delivered by two methods: a well-characterized delivery system; and a novel adaptation of a system for co-culture. When exposed to preformed $NO^{\bullet}$, a cumulative dose of 620 μM•min reduced viability of TK6 cells at 24 h to 36% and increased mutation frequencies in the *HPRT* and *TK1* genes to 7.7×10^6 ($p < 0.05$) and 24.8×10^6 ($p < 0.01$), 2.7- and 3.7-fold higher than background, respectively. In AS52 cells, cumulative doses of 1700 and 3700 μM•min reduced viability to 49% and 22%, respectively, and increased mutation frequency 10.2- and 14.6-fold higher than the argon control (132×10^6 and 190×10^6, respectively). These data show that TK6 cells were more sensitive than AS52 cells to killing by $NO^{\bullet}$. However, the two cell lines were very similar in relative susceptibility to mutagenesis; on the basis of fold-increases in MF, average relative sensitivity values [$(MF_{exp}/MF_{control})$ /cumulative $NO^{\bullet}$ dose] were 5.16×10^{-3} $\mu M^{-1}min^{-1}$, and $4.97 \times 10^{-3}\mu M^{-1}min^{-1}$ for AS52 cells.

When AS52 cells were exposed to reactive species generated by activated macrophages in the co-culture system, cell killing was greatly reduced by addition of NMA to the culture medium, and was completely abrogated by combined additions of NMA and the superoxide scavenger Tiron, indicating the relative importance of $NO^{\bullet}$ to loss of viability. Exposure in the co-culture system for 48 h increased mutation frequency in the *gpt* gene by more than 9 fold, and NMA plus Tiron again completely prevented the response. Molecular analysis of *gpt* mutants induced by preformed $NO^{\bullet}$ or by activated macrophages revealed that both doubled the frequency of gene inactivation (40% in induced vs 20% in spontaneous mutants). Sequencing showed that base-substitution mutations dominated the spectra, with transversions (30–40%) outnumbering transitions (10–20%). Virtually all mutations took place at guanine sites in the gene. G:C to T:A transversions accounted for about 30% of both spontaneous and induced mutations; G:C to A:T transitions amounted to 10–20% of mutants; insertions, small deletions and multiple mutations were present at frequencies of 0–10%. Taken together, these results indicate that cell type and proximity to generator cells are critical determinants of cytotoxic and genotoxic responses induced by $NO^{\bullet}$ and reactive species produced by activated macrophages.

*To whom correspondence should be addressed. wogan@mit.edu.

Keywords

nitric oxide; reactive oxygen species; mutation; *HPRT*; *TK1*; *gpt*

Introduction

Nitric oxide ($NO^{\bullet}$) is produced from L-arginine by $NO^{\bullet}$ synthases (NOS) at low levels by nerve and endothelial cells as a signaling molecule and at higher concentrations by activated macrophages.[1–7] $NO^{\bullet}$ rapidly reacts with superoxide anion ($O_2^{\bullet-}$) to form peroxynitrite ($ONOO^-$), a potent oxidant. $ONOO^-$ further reacts with CO_2 to form nitrosoperoxycarbonate ($ONOOCOO^-$), which decomposes into nitrogen dioxide ($NO_2^{\bullet}$) and carbonate radical ($CO_3^{-\bullet}$), also very strong oxidants. Overproduction of these reactive species in chronic inflammation can cause damage to cellular proteins, lipids and DNA, which is thought to contribute to increased genotoxicity and possibly to increased carcinogenic risk.

The complexity and extent of mutagenic responses induced by $NO^{\bullet}$ are highly dependent on steady-state levels, total cumulative dose, and types and growth mode of cells.[8] We have employed three exposure methods in attempts to create pathophysiologically relevant conditions in which to study $NO^{\bullet}$-associated genotoxicity.[9–16] We investigated genotoxicity induced by the $NO^{\bullet}$ donor SIN-1, which decomposes to release $NO^{\bullet}$, $O_2^{\bullet-}$ and $ONOO^-$, in order to mimic exposure of targets to these agents produced by macrophages, neutrophils, and endothelial cells. Exposure of TK6 (wild-type p53) and WTK-1 (mutant p53) human lymphoblastoid cells to 5 mM SIN-1 for 1.5 h increased the mutation frequency (MF) in the *HPRT* and *TK1* genes 1.7 to 2.5-fold, compared with untreated controls.[11,12] When the *supF* shuttle vector pSP189 was treated with 4 mM SIN-1 for 3 h prior to replication in *E. coli*, the mutation frequency was also increased by 3.2-fold.[14] We also examined $NO^{\bullet}$-induced mutagenesis of the *TK1* gene in TK6 (wild-type p53) and NH32 (p53 null) cells using an $NO^{\bullet}$ delivery system specifically designed to provide controlled, steady state concentrations of $NO^{\bullet}$ and molecular oxygen (O_2), mimicking the chemical environment thought to exist in inflamed tissues.[16] The MF in TK6 and NH32 cells treated with $NO^{\bullet}$ at a cytotoxic dose showed increases of 2.8- and 1.7-fold, respectively, as compared with argon-treated cells. In target cells grown in mixed cultures with mouse macrophages (RAW 264.7 cells) stimulated to produce $NO^{\bullet}$ with interferon-γ (IFN-γ) and lipopolysaccharide (LPS), we observed genotoxic responses in endogenous macrophage *HPRT* and *TK1* genes[13] as well as in human A375 cells harboring the transfected *supF* gene.[15]

The purpose of the present study was to extend the above findings to determine how delivery method, target gene structure and growth properties of cells affect mutagenic responses. As well, responses to exposure to $NO^{\bullet}$ alone and to a combination of $NO^{\bullet}$ with ROS produced by activated macrophages were evaluated. Two $NO^{\bullet}$ delivery methods were employed. In the first, $NO^{\bullet}$ and O_2 were supplied continuously into medium in a stirred chamber via diffusion through loops of gas-permeable tubing, the rates of replenishment balancing the respective rates of consumption. A model to predict $NO^{\bullet}$ and O_2 concentrations as a function of tubing lengths and delivery-gas composition has been described and verified previously,[17] and this system has been used to quantify $NO^{\bullet}$-induced cytotoxicity and mutagenesis.[6] The second delivery method involved co-culture of the target cells with activated macrophages, using a novel adaptation of the Costar Transwell™ system. The $NO^{\bullet}$-generating macrophages were cultured on the underside of the permeable support and the target cells on the top, allowing close diffusional proximity (~10 μm separation) of the cell types without physical contact, and enabling recovery of target cells after co-culture, even when both types grew as adherent monolayers. An important objective

was to evaluate the validity of this exposure system as a surrogate for *in vivo* studies in transgenic *gpt* delta mouse, which harbors the bacterial *gpt* gene as a target of mutagenic exposures. In addition, a reaction-diffusion model for predicting $NO^{\bullet}$ and O_2 concentrations generated in this system is presented here, together with a simple graphical procedure for calculating $NO^{\bullet}$ concentrations that may facilitate its application in future experiments using other cell types.

As genetic target cells that grow in adherent monolayers, we employed cells of the Chinese hamster ovary (CHO) AS52 line that carry a single copy of the *E. coli* xanthine-guanine phosphoribosyltransferase (*gpt*) gene, functionally expressed using SV40 early promoter and stably integrated into the AS52 cell genome.[18–25] AS52 cells were constructed by transfecting the plasmid vector pSV*gpt* into normal AA8 CHO cells, X-linked hypoxanthine-guanine phosphoribosyltransferase (*hprt*)-deficient, and DNA repair proficient. AS52 cells have been shown to be useful with regard to the detection of both deletion and point mutations at *gpt*, and the low spontaneous mutation fraction makes them particularly suited to quantitative and molecular mutagenesis studies. We selected these cells for several purposes: first, to characterize their mutagenic response to preformed $NO^{\bullet}$ and to activated macrophages, which has not previously been investigated; second, to evaluate genotoxicity in this co-culture system, in which target cells not in physical contact with $NO^{\bullet}$ and ROS-generating cells are exposed to diffusible reactive species; and third, as noted above, to validate this system as a potential surrogate for *in vivo* exposure of tissue cells to products of inflammatory cells. We have previously studied *gpt* mutagenesis induced in the gastric epithelium by *Helicobacter pylori* infection of the transgenic *gpt* delta mouse, which harbors multiple copies of the same bacterial *gpt* gene as AS52 Cells.[26] Information from the experiments reported here will facilitate interpretation of data from such *in vivo* experiments with respect to reactive species contributing to the observed genotoxicity.

We also used human lymphoblastoid TK6 cells, which grow in suspension, as a mutational target. Derived from a human spleen,[27, 28] they have been used extensively in mutagenicity studies.[11, 12, 16, 29, 30] The use of these two cell lines provided insights into the role of cell types, target genes (*gpt* gene of AS52, and *HPRT* and *TK1* of TK6 cells) and cell growth mode as determinants of mutagenic responses induced by $NO^{\bullet}$ and ROS. The relative contributions of $NO^{\bullet}$ and ROS to mutagenesis were assessed by employing an $NO^{\bullet}$ synthase inhibitor and ROS scavengers.

Materials and methods

Cell Cultures and Chemicals

Mouse macrophage-like RAW264.7 cells from the American Type Culture Collection (Rockville, MD) were cultured in high glucose Dulbecco's modified Eagle's medium (DMEM) containing L-glutamine supplemented with 100 units/mL penicillin, 100 μg/mL streptomycin and 10% heat-inactivated fetal bovine serum (Atlanta Biologicals, Lawrenceville, GA). TK6 cells, provided by Dr. W. G. Thilly (Massachusetts Institute of Technology), were maintained in RPMI 1640 medium supplemented as above with L-glutamine, antibiotics and 10% heat-inactivated horse serum (Lonza, Walkersville, MD). Stock cells were subcultured and maintained at densities below 1.5×10^6 cells per mL during experiments. Cells were treated with CHAT (10 μM 2′-deoxycytidine, 20 μM hypoxanthine, 0.1 μM aminopterin, and 17.5 μM thymidine) to remove pre-existent mutant cells before each experiment. Chinese hamster ovary AS52 cells, kindly provided by Dr. Helga Stopper (University of Würzburg, Germany), were grown for 7 days in Ham's F-12 medium supplemented with antibiotics and 10% heat-inactivated fetal bovine serum plus MPA supplements (10 μg/mL MPA, 250 μg/mL xanthine, 22 μg/mL adenine, 11 μg/mL thymidine and 1.2 μg/mL aminopterin) to remove pre-existing *gpt* mutants. They were

transferred to recovery medium, enriched with xanthine (11.5 μg/mL), adenine (3 μg/mL) and thymidine (1.2 μg/mL) 3 days prior to use. Cells were grown in a humidified atmosphere with 5% CO_2 in air at 37 °C.

Reagents and materials were obtained as follows: gases from Air Gas (Edison, NJ); Silastic™ tubing (0.058 in. i.d., 0.077 in. o.d.) from Dow Corning (Midland, MI); total nitrate and nitrite assay kit and recombinant mouse IFN-γ from R&D Systems (Minneapolis, MN); *N*-methyl-L-arginine monoacetate (NMA) from CalBiochem Research (Salt Lake City, UT); and *Escherichia coli* LPS (serotype 0127:B8), 4,5-dihydroxy-1,3-benzene-disulfonic acid (Tiron), uric acid, 4-nitroquinoline 1-oxide (4-NQO), 6-thioguanine(6-TG), and trifluorothymidine (TFT) and other chemicals were from Sigma (St. Louis, MO).

Exposure to preformed NO•

$NO^•$ and O_2 were delivered simultaneously into growth media of suspended and adherent target cells. This was done by diffusion through separate loops of Silastic™ tubing into a 110 mL stirred vessel.[17] The length of each tubing loop was 7 cm. TK6 cells were suspended at a density of 5×10^5 cells/mL in RPMI 1640 medium with horse serum at 37 °C, as described previously.[16] For these cells one delivery gas was 1% $NO^•$ (balance argon) and the other 50% O_2 and 5% CO_2 (balance nitrogen). The steady-state concentrations of $NO^•$ and O_2 under these conditions were calculated to be 0.7 μM (representative of inflamed tissues) and 270 μM, respectively. This calculation assumes that cellular production of $NO^•$ was negligible, which was indeed found to be true; nitrite production by both TK6 and AS52 cells was undetectable by Griess assay.

One day prior to treatment, AS52 cells were seeded at a density of 1×10^6 in 60-mm tissue culture plates to allow the cells to adhere, after which they were exposed to $NO^•$ in the same system. In this case 100% $NO^•$ was used, giving calculated concentrations of 11 μM for $NO^•$ and 82 μM for O_2. The total $NO^•$ dose delivered into the medium, expressed in units of μM•min, was controlled by varying the exposure time. Cells exposed to Ar gas under the same conditions served as negative controls. These conditions were chosen to provide steady state concentrations and cumulative doses that resulted in similar rates of cell survival (see Results). Specifically, conditions were chosen that resulted in 30%–40% survival 24 hours after exposure, because extensive experience by our group and others has shown that such conditions optimize statistical estimation of mutation frequency.

Exposure to NO• by co-culture with macrophages

Transwell™ permeable supports (Corning, NY) consist of 100 mm culture dishes, each containing a thin, porous insert of 75 mm diameter. The insert is a polycarbonate membrane with a pore diameter of 0.4 μm, a porosity of 0.13, and a thickness of 10 μm. The membrane allows rapid diffusional exchange between the cells on the top and bottom, but no direct contact between the macrophages and target cells. In co-culture experiments, RAW264.7 cells (1 mL containing 1×10^7 cells) were seeded onto the outside bottom of the membrane pretreated with medium for 1 h at 37°C, and placed in 100 mm dishes to maintain sterility. After incubation for 6 h to allow cell attachment, the medium was decanted, the membrane inverted to put the macrophages on the underside, and the co-culture unit assembled. The lower chamber of the Transwell™ device was filled with 12 mL culture medium containing 20 units/mL IFN-γ and 20 ng/mL LPS. AS52 cells suspended in 9 mL of DMEM-Ham's F-12 medium (50:50) were placed in the upper compartment, the ratio of AS52 cells to macrophages being 1:10 (1×10^6 and 1×10^7 cells, respectively). The co-cultures were incubated for 15, 24 or 48 h at 37°C in a 5% CO_2 atmosphere. After incubation, trypsinized AS52 cells were collected, washed twice, and resuspended in 10 mL of culture medium prior to analysis. Various combinations of 2 mM NMA, 1.25 mM Tiron, and 1.25 mM uric

acid were used in the lower chamber; NMA inhibits $NO^{\bullet}$ synthesis, Tiron scavenges $O_2^{\bullet -}$ and uric acid scavenges reactive products derived from $ONOO^-$, such as carbonate radical anion and nitrogen dioxide radical.

Cell viability, $NO^{\bullet}$ and $O_2^{\bullet -}$ exposure in co-culture

Cell viability 24 h after treatment was determined by trypan blue exclusion. After each period of co-culture, NO_2^- as well as the total NO_3^- plus NO_2^- content of cell supernatants were measured using a total nitrate and nitrite assay kit. Briefly, the NO_2^- concentration was determined by allowing 50 μL of culture supernatant to react with 100 μL of Griess reagent at room temperature for 10–30 min. To find the total concentration of NO_3^- plus NO_2^-, NADH and NO_3^- reductase were added before reaction with the Griess reagent, and absorbance was measured using a microplate reader at 540 nm. The concentrations were calculated from standard curves derived from standard solutions provided, with fresh culture media serving as the control.

TK6 mutation assay

After treatment, cells were maintained for 7 days to allow for phenotypic expression, then placed in selective media to determine induced MFs at the *HPRT* and *TK1* gene loci. A total of 24×10^6 cells were placed into ten 96-well microtiter plates at densities of 4×10^4 cells/well in medium containing 2 μg/mL 6-TG to select *HPRT* mutants or 2 μg/mL of TFT to select *TK1* mutants. Cells from each culture were also plated into 96-well dishes at 1 cell/100 μL/well in the absence of 6-TG or TFT to determine plating efficiency. After 2 weeks of incubation, colonies were counted and MF were calculated as described in Li *et al*[16] The spontaneous MF was estimated from the argon-treated cells for $NO^{\bullet}$ treatment or untreated cells for co-culture. Cells treated with 4-NQO, 140 ng/mL for 1.5 h served as a positive control.

AS52 mutation assay

After treatment cells were maintained in Ham's F-12 medium for expression of the mutant phenotype after treatment. At the end of incubation for 7 days, 5×10^5 cells from each group were placed in 100 mL selection medium containing 10 μM 6-TG to select *gpt* mutants and plated at 50,000 cells/10 mL/100 mm dish for determination of mutagenicity. Cells (200 cells/10 mL/100 mm dish) were grown in the absence of selecting agent for determination of plating efficiency. Colonies were scored after incubation for 2 weeks and MF was calculated from the number of 6-TG mutants.[19] Hydrogen peroxide (100 μM for 1 h) was used as a positive control mutagen. Identified *gpt* mutant colonies were then transferred to 24 well plates for propagating mutant cells. Approximately 2×10^6 mutant cells were collected for molecular analysis.

PCR amplification and molecular analysis of the gpt mutants

For analysis of the *gpt* gene, genomic DNA extracted from each mutant by using a GenElute™ mammalian genomic DNA miniprep kit was subjected to nested PCR with the following oligonucleotide primers (IDT): sense (base −199 to −181) 5'-AAGCTTGGACACAAGACAG-3' and antisense (base 520 to 540) 5'-CCAGAATACTTACTGGAAAC-3' for first round and sense (base −23 to −4) 5'-ATAAACAGGCTGGGACACTT-3' and antisense (base 460 to 479) 5'-AGTGCCAGGCGTTGAAAAGA-3' for second round PCR reaction (*31*). Two μg RNA were used as template for reverse transcriptase polymerase chain reaction (RT-PCR) with Omniscript RT kits (Qiagen, GimbH, Hilden, Germany) and the oligo(dT)15 primer (Promega, Madison, WI) provided for first-strand cDNA synthesis. The reaction was performed at 37°C for 1 h to allow the lysis of cell membrane and the synthesis of first-

strand cDNA from polyadenylated mRNA. Amplification of the cDNA was performed in two rounds of nested PCR in a PTC-200 DNA Engine Thermal Cycler (Bio-Rad, Hercules, CA). A 10 μL aliquot of cDNA solution was transferred into the first round mix of 10 μL 10×PCR buffer, 2 μL dNTP mix, 0.5 μL taq polymerase, 73.5 μL HPLC water, 0.2 μL each 25 mM forward (bases − 60 to − 41; 5'-CTGCTCCGCCACCGGCTTCC-3') and reverse (bases − 721 to − 702; 5'-GATAATTTTACTGGCGATGT-3') primer and amplified with a PCR profile of 94°C: 1 min, 30 cycles of 94°C: 1 min, 61°C: 1 min, 72°C: 1 min and a final extension of 72°C for 7 min. The product from this reaction was filtered using a Centricon 50 concentrator (Millipore, Billerica, MA) and resuspended in 100 μL sterile water to avoid unspecific binding with the remaining primers, and a 10 μL aliquot was used as template in the second round of PCR using nested primers (bases −36 to −17; 5'-CCTGAGCAGTCAGCCCGCGC-3' and bases 701 to 682; 5'-CAATAGGACTCCAGATGTTT-3'). The PCR conditions were the same in the second round as in the first-round reaction. The concentration of template DNA was 1 μg and annealing temperature 47 and 52°C. A quantity of *gpt* gene amplification was analyzed by electrophoresis on 1% agarose gels stained with ethidium bromide. The 0.5 kb PCR product was purified for DNA sequence analysis by using the QIAquick Gel Extraction Kit (Qiagen). DNA sequencing was carried out by the Dana-Farber/Harvard Cancer Center DNA Resource using 5´-ATAAACAGGCTGGGACACTT-3´ and 5´-AGTGCCAGGCGTTGAAAAGA-3´ primers (IDT).

Calculation of $NO^{\bullet}$ concentration and total exposure

For the stirred reactor, in which $NO^{\bullet}$ and O_2 delivery is by diffusion through gas-permeable tubing, concentrations and cumulative exposures were calculated using a time-dependent model that has been verified previously.[17] The initial transients were taken into account when calculating the cumulative exposures. Although for experiments using 1% $NO^{\bullet}$ gas the time to reach a steady $NO^{\bullet}$ concentration in the liquid is fairly short (12 min), for 100% $NO^{\bullet}$ that time can be appreciable (2.5 h). With 1% $NO^{\bullet}$ the concentration in the liquid overshoots the steady state value at early times; with 100% $NO^{\bullet}$ it rises monotonically to the steady value. Accordingly, the cumulative exposures reported here for 1% $NO^{\bullet}$ are somewhat larger (by 2–6%) than the steady state concentrations multiplied by the exposure times, whereas those for 100% $NO^{\bullet}$ are somewhat smaller (by 6–16%).

For the co-culture system, a novel model was developed to describe the competition between the oxidation of $NO^{\bullet}$ to NO_2^- and the diffusional loss of $NO^{\bullet}$ from the system. This allows the $NO^{\bullet}$ concentration to be calculated from the observed rate of NO_2^- accumulation in the medium. The co-culture system is shown schematically in Figure 1. The cells are placed on both sides of an insert of radius a, which fits within an outer dish of radius b. The vertical coordinate is z, with $z = -H$ at the bottom of the outer dish, $z = 0$ at the membrane, and $z = L$ at the gas-liquid interface. The porous membrane separating the macrophages (bottom of insert) from the target cells (top of insert) is thin enough (10 μm) to allow both cell layers to be viewed as residing at $z = 0$. This is the location where it is desired to know the $NO^{\bullet}$ concentration. The equations that govern the steady-state concentrations of $NO^{\bullet}$ and O_2 as functions of z are presented in the Appendix. In this apparatus the initial transient (about 20 min) was always much shorter than the total exposure (42 h), so that cumulative exposures were obtained simply by multiplying the steady-state concentrations by the exposure times.

Statistical analysis

All experiments were repeated 2–4 times. The two-tailed Student's *t*-test was used for the comparison of test and control groups, and $p < 0.05$ was considered significant.

Results

Cytotoxicity and mutagenicity of preformed NO•

Both types of target cells, TK6 and AS52, were exposed to NO• delivered by diffusion through gas-permeable tubing into the medium. When TK6 cells were exposed for 2–24 h to NO• at a steady state concentration of 0.7 μM, resulting in cumulative NO• doses ranging from 90 to 1060 μM•min, cell death was induced in a dose-dependent manner (Figure 2A). A comparable response in AS52 cells required treatment for 1, 2, 3, 6 and 8 h with NO• at a steady-state concentration of 11 μM, producing cumulative total doses of 533, 1067, 1700, 3700, and 5040 μM•min (Figure 2A). Thus, AS52 cells were substantially more resistant than TK6 cells to NO•-induced cytotoxicity; cell viability was 36% in TK6 cells 24 h after a dose of 620 μM•min NO•, compared to 49 and 22% in AS52 cells after treatment with 1700 and 3700 μM•min, respectively (arrows in Figure 2A).

Mutagenicity of NO• in the *HPRT* and *TK1* genes of TK6 cells and *gpt* gene of AS52 cells was also investigated (Figure 2B and C). As indicated in the Figure and in Materials and Methods, cumulative NO• doses permitting 20%–50% survival were chosen in order to optimize mutagenic responses. At a cumulative dose at 24 h of 620 μM•min, induced mutation frequencies in the *HPRT* and *TK1* genes were 7.7×10^6 ($p < 0.05$) and 24.8×10^6 ($p < 0.01$), 2.7- and 3.7-fold higher than background (2.9×10^6 and 6.7×10^6), respectively (Figure 2B). By comparison, in 4-NQO-treated positive controls, mutation frequencies at the *HPRT* and *TK1* loci were 14.6×10^6 and 28.1×10^6, respectively (Figure 2B). In AS52 cells, exposure to 1700 and 3700 μM•min NO• also resulted in a dose-dependent increase in MF (132×10^6 and 190×10^6, respectively), 10.2- and 14.6-fold higher ($p < 0.01$) than the argon control, (MF, 13×10^6) (Figure 2C). The MF in the positive control AS52 cells treated with 100 μM H_2O_2 for 1 h was 210×10^6. Thus, with respect to relative susceptibility to mutagenesis defined as [($MF_{exp}/MF_{control}$) /cumulative NO• dose], the two cell lines were very similar. On the basis of fold-increases in MF, average relative sensitivity values were 5.16×10^{-3} $M^{-1}min^{-1}$and $4.97 \times 10^{-3}\mu M^{-1}min^{-1}$ for AS52 cells.

Viability and mutagenesis in AS52 cells co-cultivated with activated macrophages

A time-dependent decrease in the viability of AS52 cells co-cultivated with macrophages is shown in Table 1. Stimulated macrophages reduced the number of surviving cells to 26% at 48 h, whereas inhibition of NO• synthesis with NMA restored the cell survival to a rate near that of controls (83%). Addition of both NMA and the superoxide scavenger Tiron increased survival rates even closer to controls (94%), suggesting that species derived from superoxide anion played a significant role in cell killing in addition to that of NO•. Inclusion of uric acid (a scavenger of reactive products derived from peroxynitrite) in the medium, in addition to NMA and Tiron, had no additional effect in addition to NO• on viability. In the absence of macrophage activation, NMA alone had no effect on viability (data not shown).

A time-dependent increase in MF of the *gpt* gene was observed in the presence of activated macrophages. The MF induced by exposure for 48 h, 170×10^{-6}, was 9.4-fold higher than the background MF, 18×10^{-6} (Table 1). Whereas NMA did not restore MF completely to control levels, the combination of NMA and Tiron (with or without uric acid) resulted in a MF not statistically different than that of controls. The roughly ten-fold increase in MF of the *gpt* gene in co-culture is similar to that observed in the experiments with preformed NO•.

Nitrite and nitrate production in co-culture

Activation of RAW264.7 cells increased the production of NO_2^-, a marker for NO• biosynthesis (Table 1). The potent macrophage activators IFN-γ and LPS caused the NO_2^- concentration at 48 h to be almost 30-fold higher than in controls (127 vs. 4.5 μM). There

was a similarly large increase in the total NO_2^- plus NO_3^- concentration at 48 h (170 vs. 7.9 μM). NMA strongly affected the production of NO_2^-, reducing its concentration at 48 h to 16 μM, whereas the presence also of Tiron or uric acid had little or no additional effect (Table 1).

NO• concentration and dose in co-culture

The reaction-diffusion model described in the Appendix was used to calculate NO• concentrations and doses in the co-culture experiments, based on the observed rates of NO_2^- accumulation. The need for such a model is illustrated in Figure 3, which shows the diffusional losses of NO• predicted for varying rates of NO• synthesis. Results are shown for three levels of respiratory O_2 consumption by the cells, the consumption being negligible for $A = 0$ and maximal for $A = 1$. (The estimation of this quantity for our experiments will be discussed shortly.) As shown in Figure 3, the smaller the rate of NO• synthesis, the greater is the percentage loss of NO• by diffusion out of the liquid. Also, the loss of NO• is increased if the availability of O_2 is reduced by increasing A. Decreasing the NO• concentration by decreasing its rate of synthesis, or decreasing the O_2 concentration by increasing its consumption by cells, slows the trapping of NO• by oxidation to NO_2^-. Because the rate of autoxidation depends on the square of the NO• concentration [Eq. (A2)] and diffusion is proportional only to the first power, diffusional losses increasingly predominate as the concentration is decreased. At physiological concentrations, where most of the NO• may be lost by diffusion, the rate of accumulation of NO_2^- (or NO_2^- plus NO_3^-) may greatly underestimate the rate of NO• biosynthesis. Moreover, the rate of NO_2^-accumulation is not a fixed fraction of the rate of NO• synthesis, so that proportionality cannot be assumed.

To estimate NO• concentrations in the co-culture experiments, average rates of NO_2^- accumulation were found by subtracting the control NO_2^- concentration from that at 48 h, and dividing the concentration difference by 42 h. This assumes an induction period of 6 h for NO• synthase.[32] These calculations, detailed in the Appendix, required that the rate of respiratory consumption of O_2 be estimated. The parameter which varies with the numbers and types of cells in a given experiment is R_{max}, the maximum rate of O_2 consumption [Eq. (A20)]. The initial numbers of AS52 and RAW264.7 cells were 1×10^6 and 1×10^7, respectively, and these were co-cultured for 48 h prior to any measurements. As already mentioned, it was found that 26% of the AS52 cells were viable in the absence of NOS inhibitor and 83% were viable with NMA present. Based on previous results for RAW264.7 cells at similarly high cell numbers (*33*), the corresponding values were 12% without NMA and 24% with NMA. Using the respective doubling times of 19 h (*34*) and 22 h (*33*), we estimate the numbers of viable cells at 48 h as $m_T = 1.5 \times 10^6$ (AS52, target cells) and $m_G = 5.4 \times 10^6$ (RAW264.7, generator cells). Combining these cell numbers with maximum respiration rates of 60 pmol s^{-1} $(10^6 \text{ cells})^{-1}$ for AS52 (*35*) and 100 pmol s^{-1} $(10^6 \text{ cells})^{-1}$ for RAW264.7 (*36*), $R_{max} = 1.4 \times 10^{-7}$ mol m^{-2} s^{-1}. From Eqs. (A21) and (A22), the initial estimate for the O_2 consumption parameter was then $A_0 = 0.48$. For the experiments without inhibition of NOS, the increase in NO_2^- concentration of 123 μM over 42 h corresponds to an accumulation rate of $R = 0.81$ nM/s. The final value of the O_2 consumption parameter obtained via the iterative procedure described in the Appendix was $A = 0.15$, and the cellular NO• concentration was 1.05 μM (Table 1). The net rate of NO• synthesis was calculated as $N = 3.7 \times 10^{-9}$ mol m^{-2} s^{-1}, corresponding to a value of $B = 4.3$ for the NO• reaction-diffusion parameter. For the experiments with NMA, $R = 0.076$ nM/s, $A = 0.47$, $C_{NO}(0) = 0.36$ μM, $N = 0.74 \times 10^{-9}$ mol m^{-2} s^{-1}, and $B = 0.85$. Thus, although the rate of NO_2^- accumulation with NMA was only 9% of that without NOS inhibition, the NO• concentration was 34% of that without inhibition. This disproportionality is a consequence of the nonlinear dependence of the autoxidation rate on the concentration of NO• [Eq. (A2)].

In the experiments where Tiron or uric acid were included in addition to NMA, the estimated $NO^{\bullet}$ concentration again was about 0.3 μM (Table 1).

Also shown in Table 1 are the total $NO^{\bullet}$ doses in the co-culture experiments. The addition of NMA reduced the cumulative exposure of the AS52 cells by about two-thirds (from 2650 to 810–910 μM•min), paralleling the reduction in $NO^{\bullet}$ concentration. The fraction of synthesized $NO^{\bullet}$ lost from the system was estimated as 36% without NOS inhibition and 70–73% with NMA, emphasizing the need to account for diffusional losses. At 48 h and without NOS inhibition, the viability of AS52 cells in co-culture was slightly lower than for exposure to preformed $NO^{\bullet}$ at the same dose (Figure 2A).

Molecular analysis of gpt mutants

A total of 22 and 51 6-TG resistant mutants isolated from AS52 cells exposed in co-culture to unactivated and activated macrophages, respectively, were initially characterized by PCR to determine the presence of the intact *gpt* gene (0.5 kb PCR product) and non-coding rearrangements of the pSV2 *gpt* plasmid sequences (0.8 kb PCR product). Loss or alteration of one or both bands suggested more complex chromosomal deletions and/or rearrangements inactivating the *gpt* gene (37). This analysis showed that the *gpt* gene was deleted or structurally rearranged in 23% and 40% of mutants occurring after exposure to unactivated and IFN-γ/LPS-activated macrophages, respectively (Table 2). When present, PCR-amplified products of structural *gpt* gene sequences were isolated and sequenced, with results summarized in Table 3. After exposure to unactivated macrophages, the majority of mutations identified were single base pair substitutions (35%) and deletions (53%); other mutations included single base pair insertions (6%) and multiple mutations (6%). In mutants induced by exposure to activated macrophages, the major form was again single base-pair substitution, but at a higher proportion (66%), with deletions occurring at lower frequency (20%). Multiple sequence changes were also detected in 6% and 7% of cells exposed to unactivated and activated macrophages, respectively.

In mutants from all co-culture treatment groups, G:C to T:A transversions were the predominating type of single base-substitution, with frequencies of 29% in unactivated and 33% in activated macrophage treatment groups, respectively. As also shown in Table 3, single base pair substitutions predominated (56%) in mutants induced by exposure to preformed $NO^{\bullet}$; G:C to T:A transversions were present in 29%, followed by A:T to C:G transversions (10%), G:C to A:T transitions (10%) and A:T to T:A transversions (3%). Whereas the proportions of single base-pair substitutions were similar, G:C to A:T transitions (20%) were much more frequent following exposure of target cells to co-culture with activated macrophages.

Positions of sequence changes induced in the *gpt* gene of AS52 cells by the exposure scenarios used are presented in Supplemental Tables 1 and 2. No “hot spots” for any type of mutation were identified in the induced mutants, except for single base deletions at base 30 and three base deletions at bases 369–371, which were common in both induced and negative control mutants; these are inherent in the assay system, as shown by many previous investigators. Otherwise, the most numerous changes observed were five base substitutions occurring at positions 413 and 414 following IFN-γ/LPS treatment by co-culture, with remaining mutations distributed across most of the gene sequence.

Discussion

We studied the effects of $NO^{\bullet}$ and ROS on cell viability and mutagenesis using two experimental systems: a stirred chamber in which pre-formed $NO^{\bullet}$ diffused into the culture media from gas-permeable tubing,[16, 17] and a novel co-culture system in which target cells

were physically separated from $NO^{\bullet}$-generating macrophages, enabling detection of mutations induced by diffusible agents. In both systems, a steady $NO^{\bullet}$ concentration could be maintained for up to 48 h (the longest period examined), and the $NO^{\bullet}$ concentration and cumulative dose received by the target cells could be quantified. We also employed two mammalian gene mutation assay systems, suspended TK6 cells (*HPRT* and *TK1* genes) and adherent AS52 cells (*gpt* gene), to investigate how $NO^{\bullet}$ and ROS mutagenicity was affected by target genes, cell types and growth mode.

The major findings of these experiments can be summarized briefly as follows. When exposed to preformed $NO^{\bullet}$, TK6 cells proved to be more sensitive to cell killing than AS52 cells; equivalent reductions in viability were caused by cumulative doses of 1060 vs 3700 μM•min, respectively. On the other hand, the two cell types were equally sensitive to the mutagenic effects of $NO^{\bullet}$. When AS52 cells were exposed to reactive species generated by activated macrophages in the co-culture system, cell killing was greatly reduced by addition of NMA to the culture medium, and was completely abrogated by combined additions of NMA and the ROS scavenger Tiron, indicating the relative importance of $NO^{\bullet}$ to loss of viability. Exposure in the co-culture system for 48 h increased mutation frequency in the *gpt* gene by more than 9 fold, and NMA plus Tiron again completely prevented the response. Molecular analysis of *gpt* mutants induced by preformed $NO^{\bullet}$ or by activated macrophages revealed that both doubled the frequency of gene inactivation (40% in induced vs 20% in spontaneous mutants). Sequencing showed that base-substitution mutations dominated the spectra, with transversions (30–40%) outnumbering transitions (10–20%). Virtually all mutations took place at guanine sites in the gene. G:C to T:A transversions accounted for about 30% of both spontaneous and induced mutations; G:C to A:T transitions amounted to 10–20% of mutants; insertions, small deletions and multiple mutations were present at frequencies of 0–10%.

Responses to exposures via the co-culture format used in the current experiments in which macrophages are physically separated from genetic targets, requiring diffusion of genotoxic products, have not previously been described. Importantly, when compared at the same total dose, viability loss was quite similar in AS52 cells exposed to pre-formed $NO^{\bullet}$ or to the co-culture system, again indicating the importance of $NO^{\bullet}$ in eliciting cytotoxicity and its diffusivity from generator to target cells. It is of interest to compare these findings with data obtained in our previous studies in which the endogenous *hprt* gene of CHO-AA8 cells (parents of AS52 cells) served as the genetic target.[9] A highly significant increase was induced in *HPRT* MF in cells grown in mixed cultures with activated macrophages in which generator and target cells were in direct physical contact; NMA blocked approximately 90% of nitrite production and cytotoxicity in cells exposed for 26 hours, but only 40% in those co-cultured for 36 hours. A significant increase in mutation frequency was observed only in cells exposed for 36 hours, and the increase was only partially abrogated by NMA, probably reflecting concurrent production of other cytotoxic and genotoxic agents by stimulated macrophages in addition to $NO^{\bullet}$.

In another earlier study, we characterized mutagenesis in the target *supF* gene of pSP189 replicating in AD293 cells grown in mixed culture with activated macrophages, which were shown to produce substantial amounts of $NO^{\bullet}$, $O_2^{\bullet-}$ and hydrogen peroxide (H_2O_2) over 12–72 h periods. After 72 h, a 3.7-fold increase in *supF* MF was observed, and co-treatment with NMA, superoxide dismutase and catalase suppressed mutagenesis by 87%. Analysis of mutation spectra revealed that single base pair substitutions were prevalent (70% –85%), almost all of which occurred at G:C base pairs, and consisted predominantly of G:C to T:A transversions. Collectively these results strongly suggested that $ONOO^-$ or its derivatives, generated by reaction of $NO^{\bullet}$ with $O_2^{\bullet-}$, may have been a major contributor to mutagenesis by activated macrophages in this system.

As noted above, a main purpose of the present study was to evaluate responses in the AS52 cell model as surrogates for *in vivo* studies of genotoxicity resulting from chronic inflammation. It is particularly informative in this connection to compare these findings with those of a recently completed study in which we characterized mutations induced in gastric tissue of the *gpt* delta mouse infected with *Helicobacter pylori*, which has been classified by IARC as a known human carcinogen on the basis of its impact on gastric cancer.[26] We used the *gpt* delta mouse to measure the accumulation of gastric mutations associated with *H. pylori* infection in animals at 6 and 12 months post infection. As noted above, these mice harbor tandem arrays of 80 copies of the bacterial *gpt* gene (the same reporter gene as AS52 cells) at a single site on chromosome 17. Point mutations were increased in females infected for 12 months; mutation frequency in this group was significantly higher than in uninfected mice of both sexes. A:T-to-G:C transitions and G:C-to-T:A transversions were 3.8 and 2.0 times, respectively, more frequent in this group than in controls. Relative frequencies of these two mutations are similar in many respects to those induced in AS52 cells by exposure to pre-formed $NO^{\bullet}$ and co-culture with activated macrophages, in that they consist primarily of transversions located at guanine sites, and are consistent with the expected mutational spectrum induced by reactive oxygen and nitrogen species (RONS). An important difference, however, is the large fraction of transversions located at adenine sites, which were not prominent in the *in vitro* system. A:T-to-G:C transitions can be formed by deamination of adenine, mediated by N_2O_3, an autoxidation product of $NO^{\bullet}$, to hypoxanthine, which mispairs with cytosine, resulting in the observed mutation. Alternatively, A:T-to-G:C transitions can also be created indirectly by lipid peroxidation by RONS, forming highly mutagenic ethenoadenine. This difference between the *in vivo* and *in vitro* findings suggests that lipid peroxidation may be an important determinant of mutagenesis in intact animals, but not in cultured cells.

In the present experiments, both exposure to pre-formed $NO^{\bullet}$ and co-cultivation with $NO^{\bullet}$-producing macrophages caused cell killing and mutagenicity in AS52 cells. $NO^{\bullet}$ has been shown to mediate cell death through a number of mechanisms, including induction of apoptosis, energy depletion resulting from acotinase inhibition, lipid oxidation, DNA strand breaks, and possibly protein modification through nitrotyrosine formation.[38] TK6 cells were more sensitive than AS52 cells to $NO^{\bullet}$-mediated killing, which may result from differences in susceptibility to induction of apoptosis, and may also reflect differences in intracellular levels of antioxidant defense mechanisms in the two target cell lines. Although responsible mechanisms are not known, it is noteworthy that TK6 cells were exposed in suspension culture whereas AS52 cells grew as adherent monolayers. Collectively, the above data support the interpretation that genotoxicity induced by activated immune cells results from increased production of multiple reactive species, including nitric oxide ($NO^{\bullet}$), $O_2^{\bullet-}$, H_2O_2, $ONOO^-$ and nitrous anhydride (N_2O_3) *in vitro* and *in vivo*. Compared to $NO^{\bullet}$, superoxide has a much shorter half-life (<50 milliseconds) and a free diffusion path of only 2 μm, and thus in the co-culture system may have had a smaller impact on mutagenicity. This conclusion is supported by observations that inhibition of $NO^{\bullet}$ production by the NOS inhibitor NMA reduced genotoxicity by 70%–80% in co-culture experiments.

The $NO^{\bullet}$ concentrations experienced by cells in the co-culture system can be calculated from measured rates of NO_2^- accumulation by solving the differential equations in the Appendix. Alternatively, they can be found using a simple graphical procedure based on Fig. 4. The $NO^{\bullet}$ concentration at the level of the cells [$C_{NO}(0)$] is plotted as a function of the NO_2^- formation rate (R) for several values of the O_2 consumption parameter (A) and a liquid depth of 2 mm in the upper chamber. To find $C_{NO}(0)$ from a measured value of R, the first step is to obtain an initial value for A. This requires knowledge of the numbers of viable cells and measured or estimated values of their maximum rates of O_2 consumption, as detailed for the present experiments in the Results section. By choosing the curve in Fig. 4 that corresponds

to this initial value of A, a first estimate of $C_{NO}(0)$ is found from R. To refine the estimated concentration, the parameters β and γ are calculated from Eq. (A22). Whereas β is the same for all such experiments, γ depends on $C_{NO}(0)$. The value of A is refined using $A/A_0 = (1 + \beta)/(1 + \beta + \gamma)$. Using the improved value of A, $C_{NO}(0)$ is updated by returning to Fig. 4. This procedure converges rapidly enough that only 1–2 updates of $C_{NO}(0)$ are usually needed. When the graphical method was applied to the present data without NOS inhibition, two-digit accuracy [$C_{NO}(0) = 1.0$ mM] was obtained with just one update. Although Fig. 4 assumes an upper chamber depth of $L = 2$ mm, satisfactory estimates can be obtained also for other depths. If $A \leq 0.6$, as is likely, we recommend that $C_{NO}(0)$ found from Fig. 4 be increased by 15% if $L = 3$ mm and decreased by 24% if $L = 1$ mm. (The precise correction factors range from a 13–18% increase for $L = 3$ mm to a 21–27% decrease for $L = 1$ mm, depending on the value of R.)

Acknowledgments

This work was supported by National Cancer Institute Grants No. 5 P01 CA26731 and R01 9CA095039, NIEHS Center Grant ES02109, and MIT Center for Environmental Health Sciences NIEHS P30 ES002109-26A1.

Abbreviations

gpt	*E. coli* xanthine-guanine phosphoribosyltransferase
HPRT	hypoxanthine phosphoribosyltransferase
IFN-γ	interferon-γ
LPS	lipopolysaccharide
MF	mutation frequency
NMA	*N*-methyl-L-arginine monoacetate
ROS	reactive oxygen species
SOD	superoxide dismutase
TK1	thymidine kinase 1

Appendix: Co-culture Model

Assumptions

The co-culture system was represented as in Fig. 1. There are two pathways for entry of O_2 and loss of $NO^{\bullet}$ from the stagnant liquid. One is diffusion directly above the insert. A less direct route combines radial diffusion within the bottom chamber with vertical diffusion in the annular space between the insert and dish. The resistance of the second pathway relative to the first is approximately $a^2/(4HL) = 180$, where a (= 37.5 mm) is the radius of the insert, H (= 1 mm) is the depth of the lower chamber, and L (= 2 mm) is the liquid depth in the upper chamber. Accordingly, the second pathway was neglected. A steady-state model is appropriate because the time required for diffusion of either species across a 2 mm film (L^2/D = 20 min) is much shorter than the duration of the experiments (48 h). Accordingly, concentrations were assumed to be functions of z only. The concentration of species i is denoted as $C_i(z)$.

Competing with the diffusional loss of $NO^{\bullet}$ to the incubator gas is its reaction with O_2.

The multistep autoxidation of $NO^{\bullet}$ is written overall as (*39*)

$$4NO+O_2+2H_2O \xrightarrow{k} 4NO_2^-+4H^+. \quad \text{(A1)}$$

The rate constant k is defined such that the local rate of formation of NO_2^- per unit volume is

$$R_V=\frac{dC_{NO_2^-}}{dt}=4kC_{NO}^2C_{O_2}. \quad \text{(A2)}$$

This is also the rate of consumption of NO• by autoxidation, whereas the rate of O_2 consumption in the medium is $R_V/4$. The measurable quantity is the average of R_V over the entire liquid volume, which is denoted as R.

Oxygen is plentiful enough and autoxidation slow enough that the effect of autoxidation on C_{O_2} is negligible. However, cellular consumption by respiration can be an important sink for O_2. Because NO• inhibits respiration and O_2 is needed to trap NO• as NO_2^-, the concentrations of NO• and O_2 are linked. In what follows, the governing equations will be stated, the parameters that affect $C_{O_2}(z)$ and $C_{NO}(z)$ defined, and the solution procedure described. How the model can be used to infer the cellular NO• concentration from measurements of R will be explained.

Governing equations

The differential equations which describe the O_2 and NO• concentrations are those used previously in modeling macrophage cultures.[40] What distinguishes the present system are the boundary conditions. The O_2 concentration in the medium is governed by

$$\frac{d^2C_{O_2}}{dz^2}=0 \quad \text{(A3)}$$

which is subject to the conditions

$$\frac{dC_{O_2}}{dz}(-H)=0 \quad \text{(A4)}$$

$$-D_{O_2}\frac{dC_{O_2}}{dz}(0^-)+D_{O_2}\frac{dC_{O_2}}{dz}(0^+)=M \quad \text{(A5)}$$

$$C_{O_2}(L)=C_0 \quad \text{(A6)}$$

Equation (A4) expresses the assumption that the bottom of the dish ($z = -H$) is impermeable to O_2 and Eq. (A6) equates the concentration at the top surface ($z = L$) with C_0, the aqueous value in equilibrium with the incubator gas. In Eq. (A5) the net flux toward the membrane (at $z = 0$) is equated with the rate of cellular O_2 consumption. Here, D_{O_2} is the aqueous diffusivity and M is the total rate of O_2 consumption per unit area of insert (e.g., mol m^{-2} s^{-1}). As will be described, M depends on both the O_2 and the NO• concentrations.

The solution to Eq. (A3) that satisfies Eqs. (A4)–(A6) is

$$C_{O_2}(z)=C_0+\frac{M}{D_{O_2}}(z-L) \quad (0 \le z \le L) \tag{A7a}$$

$$C_{O_2}(z)=C_0-\frac{ML}{D_{O_2}} \quad (-H \le z \le 0) \tag{A7b}$$

As shown, the O_2 concentration in the upper chamber increases linearly with height, whereas that in the lower chamber is constant.

The $NO^{\bullet}$ concentration is influenced significantly by autoxidation. The differential equation for $NO^{\bullet}$ is

$$D_{NO}\frac{d^2C_{NO}}{dz^2}=4k_1C_{NO}^2C_{O_2} \tag{A8}$$

and the boundary conditions are

$$\frac{dC_{NO}}{dz}(-H)=0 \tag{A9}$$

$$D_{NO}\frac{dC_{NO}}{dz}(0^-)-D_{NO}\frac{dC_{NO}}{dz}(0^+)=N \tag{A10}$$

$$C_{NO}(L)=0 \tag{A11}$$

Here the total flux away from the membrane equals N, the net rate of cellular $NO^{\cdot}$ production per unit area, and $NO^{\cdot}$ is assumed to be absent from the incubator gas. The value of N reflects $NO^{\cdot}$ synthesis by the macrophages minus consumption by either cell type. A consequence of the localized source is that $C_{NO}(z)$ is greatest at $z = 0$.

Scaled dimensionless variables were employed to minimize the number of parameters and simplify the numerical solution. The dimensionless position and $NO^{\cdot}$ concentrations are

$$\zeta=\frac{z}{L}, \quad \theta=\frac{C_{NO}D_{NO}}{NL}. \tag{A12}$$

Substitution of Eq. (A7) into Eq. (A8) and changing to dimensionless variables gives

$$\frac{d^2\theta}{d\zeta^2}=B\left[1+A(\zeta-1)\right]\theta^2 \quad (0 \le \zeta \le 1) \tag{A13}$$

$$\frac{d^2\theta}{d\zeta^2}=B(1-A)\theta^2 \quad (-H/L \le \zeta \le 0) \tag{A14}$$

$$A=\frac{ML}{D_{O_2}C_0}, \quad B=\frac{4kC_0NL^3}{D_{NO}^2} \quad . \tag{A15}$$

The differential equations now contain just two parameters: A is cellular O_2 consumption relative to the maximum possible O_2 flux in the upper chamber ($0 \le A \le 1$); and B is the rate

of autoxidation of NO˙ relative to its rate of diffusion. In our experiments the one additional parameter, *H/L*, was fixed at 0.5. The dimensionless boundary conditions are

$$\frac{d\theta}{d\zeta}(-H/L)=0 \tag{A16}$$

$$\frac{d\theta}{d\zeta}(0^-) - \frac{d\theta}{d\zeta}(0^+)=1 \tag{A17}$$

$$\theta(1)=0. \tag{A18}$$

What remains to be described are the effects of O_2 and NO˙ on respiration, which influences the evaluation of the O_2 consumption parameter, *A*.

Oxygen consumption parameter

Taking into account the effects of O_2 limitations and NO˙ inhibition on respiration, the O_2 consumption rate is expressed as

$$M=\frac{R_{\max}C_{O_2}(0)}{C_{O_2}(0)+K_M[1+C_{NO}(0)/K_I]} \tag{A19}$$

where R_{max} is the maximum rate of O_2 consumption per unit area and K_M and K_I are constants.[36] Using "G" and "T" to denote NO˙ generator cells (macrophages) and target cells (AS52), respectively,

$$R_{\max}=\frac{m_G R_{\max,G}+m_T R_{\max,T}}{\pi a^2} \tag{A20}$$

where m_i is the number of viable cells of type *i* and $R_{max,i}$ is the maximum rate of O_2 consumption for that cell type. The values of K_M and K_I should be similar for all cells, as they are properties of the respiratory enzymes. Likewise, R_{max} can be calculated from the numbers of viable cells and rates of O_2 consumption from the literature. Thus, the main reason that *M* (and thus *A*) is not known in advance is that it depends on the unknown O_2 and NO˙ concentrations at $z = 0$.

Using Eq. (A7b) to eliminate $C_{O_2}(0)$ from Eq. (A19) leads to a quadratic equation for *M*. Choosing the root that yields positive values of $C_{O_2}(0)$, the O_2 consumption parameter is evaluated as

$$A=\frac{1+\alpha+\beta+\gamma}{2}\left[1-\sqrt{1-\frac{4\alpha}{(1+\alpha+\beta+\gamma)^2}}\right] \tag{A21}$$

$$\alpha=\frac{R_{\max}L}{D_{O_2}C_0},\beta=\frac{K_M}{C_0},\gamma=\frac{K_M C_{NO}(0)}{K_I C_0}=\frac{BK_M D_{NO}}{4kC_0^2K_I L^2}\theta(0). \tag{A22}$$

Whereas α and β are constants, γ causes *A* to depend on the calculated NO˙ concentration profile. In the absence of NO˙ (i.e., for $\gamma = 0$), *A* has a maximum value denoted as A_0.

Solution procedure

Equations (A13) and (A14) were solved numerically for both regions using Maple 12 (Maplesoft, Waterloo, Ontario, Canada). It was assumed initially that $A = A_0$, and then the value of A was refined using an iterative procedure. The algorithm depended on whether or not the rate of $NO^{\bullet}$ production, and therefore the value of B, was known. If B was given, Eqs. (A13) and (A14) were solved repeatedly, adjusting $\theta(0)$ until Eq. (A17) was satisfied to within 0.01 %. If the left-hand side of Eq. (A17) was larger than 1, it was necessary to decrease $\theta(0)$, and vice versa. Equation (A21) was then used to find a new value of A. Usually, only 1–3 adjustments of A were needed for it to converge to within 1%.

When inferring the cellular $NO^{\cdot}$ concentration from the measured rate of NO_2^- formation, R was given but B was unknown. For these cases an initial guess for B was made and then the above procedure was followed until the convergence of A was satisfactory. A new value of B was calculated from the current solution using

$$B=\frac{L^2}{D_{NO}}\sqrt{\frac{4kC_0R}{J}} \tag{A23}$$

$$J=\left(\frac{L}{H+L}\right)(1-A)\int_{-H/L}^{0}\theta^2 d\zeta+\left(\frac{L}{H+L}\right)\left[(1-A)\int_{0}^{1}\theta^2 d\zeta+A\int_{0}^{1}\theta^2\zeta d\zeta\right] \tag{A24}$$

where J is the dimensionless rate of autoxidation obtained from the $NO^{\cdot}$ and O_2 concentration profiles in the two chambers. If B from Eq. (A23) differed from the trial value by more than 1%, it was used as the new trial value and the procedure repeated. Typically, the convergence was satisfactory after 2–3 iterations. An initial guess for B can be obtained from Eqs. (A23) and (A24) by assuming that $\theta(\zeta) = 1$ in the lower chamber and $\theta(\zeta) = 1 - \zeta$ in the upper one.

The physicochemical parameters used in these calculations are $k = 2.4 \times 10^6\ M^{-2}\ s^{-1}$ (39), $C_0 = 200\ \mu M$ (41), $D_{NO} = 3.0 \times 10^{-9}\ m^2\ s^{-1}$ (42), $D_{O2} = 2.8 \times 10^{-9}\ m^2\ s^{-1}$ (43), and $K_M = 7\ \mu M$ (36).

References

1. Chanock SJ, el Benna J, et al. The respiratory burst oxidase. J Biol Chem. 1994; 269(40):24519–24522. [PubMed: 7929117]
2. Ohshima H, Bartsch H. Chronic infections and inflammatory processes as cancer risk factors: possible role of nitric oxide in carcinogenesis. Mutat Res. 1994; 305(2):253–264. [PubMed: 7510036]
3. Czapski G, Goldstein S. The role of the reactions of .NO with superoxide and oxygen in biological systems: a kinetic approach. Free Radic Biol Med. 1995; 19(6):785–794. [PubMed: 8582651]
4. Wiseman H, Halliwell B. Damage to DNA by reactive oxygen and nitrogen species: role in inflammatory disease and progression to cancer. Biochem J. 1996; 313(Pt 1):17–29. [PubMed: 8546679]
5. MacMicking J, Xie QW, et al. Nitric oxide and macrophage function. Annu Rev Immunol. 1997; 15:323–350. [PubMed: 9143691]
6. Vamvakas S, Schmidt HH. Just say NO to cancer? J Natl Cancer Inst. 1997; 89(6):406–407. [PubMed: 9091635]
7. Ohshima H, Tatemichi M, et al. Chemical basis of inflammation-induced carcinogenesis. Arch Biochem Biophys. 2003; 417(1):3–11. [PubMed: 12921773]

8. Li CQ, Wogan GN. Nitric oxide as a modulator of apoptosis. Cancer Lett. 2005; 226(1):1–15. [PubMed: 16004928]
9. Zhuang JC, Lin C, et al. Mutagenesis associated with nitric oxide production in macrophages. Proc Natl Acad Sci U S A. 1998; 95(14):8286–8291. [PubMed: 9653179]
10. Zhuang JC, Wright TL, et al. Nitric oxide-induced mutations in the HPRT gene of human lymphoblastoid TK6 cells and in Salmonella typhimurium. Environ Mol Mutagen. 2000; 35(1): 39–47. [PubMed: 10692226]
11. Li CQ, Trudel LJ, et al. Genotoxicity, mitochondrial damage, and apoptosis in human lymphoblastoid cells exposed to peroxynitrite generated from SIN-1. Chem Res Toxicol. 2002; 15(4):527–535. [PubMed: 11952339]
12. Li CQ, Trudel LJ, et al. Nitric oxide-induced genotoxicity, mitochondrial damage, and apoptosis in human lymphoblastoid cells expressing wild-type and mutant p53. Proc Natl Acad Sci U S A. 2002; 99(16):10364–10369. [PubMed: 12136132]
13. Zhuang JC, Lin D, et al. Genotoxicity associated with NO production in macrophages and co-cultured target cells. Free Radic Biol Med. 2002; 33(1):94–102. [PubMed: 12086687]
14. Kim MY, Dong M, et al. Effects of peroxynitrite dose and dose rate on DNA damage and mutation in the supF shuttle vector. Chem Res Toxicol. 2005; 18(1):76–86. [PubMed: 15651852]
15. Kim MY, Wogan GN. Mutagenesis of the supF gene of pSP189 replicating in AD293 cells cocultivated with activated macrophages: roles of nitric oxide and reactive oxygen species. Chem Res Toxicol. 2006; 19(11):1483–1491. [PubMed: 17112236]
16. Li CQ, Pang B, et al. Threshold effects of nitric oxide-induced toxicity and cellular responses in wild-type and p53-null human lymphoblastoid cells. Chem Res Toxicol. 2006; 19(3):399–406. [PubMed: 16544944]
17. Wang C, Deen WM. Nitric oxide delivery system for cell culture studies. Ann Biomed Eng. 2003; 31(1):65–79. [PubMed: 12572657]
18. Tindall KR, Stankowski LF Jr, et al. Detection of deletion mutations in pSV2gpt-transformed cells. Mol Cell Biol. 1984; 4(7):1411–1415. [PubMed: 6095070]
19. Hsie AW, Recio L, et al. Evidence for reactive oxygen species inducing mutations in mammalian cells. Proc Natl Acad Sci U S A. 1986; 83(24):9616–9620. [PubMed: 2432598]
20. Tindall KR, Stankowski LF Jr, et al. Analyses of mutation in pSV2gpt-transformed CHO cells. Mutat Res. 1986; 160(2):121–131. [PubMed: 3005850]
21. Tindall KR, Stankowski LF Jr. Molecular analysis of spontaneous mutations at the gpt locus in Chinese hamster ovary (AS52) cells. Mutat Res. 1989; 220(2–3):241–253. [PubMed: 2494446]
22. Ariza ME, Williams MV. Mutagenesis of AS52 cells by low concentrations of lead(II) and mercury(II). Environ Mol Mutagen. 1996; 27(1):30–33. [PubMed: 8625945]
23. Ariza ME, Bijur GN, et al. Lead and mercury mutagenesis: role of H_2O_2, superoxide dismutase, and xanthine oxidase. Environ Mol Mutagen. 1998; 31(4):352–361. [PubMed: 9654245]
24. Jiwajinda S, Santisopasri V, et al. Suppressive effects of edible Thai plants on superoxide and nitric oxide generation. Asian Pac J Cancer Prev. 2002; 3(3):215–223. [PubMed: 12718578]
25. Kim HW, Murakami A, et al. Suppressive effects of selected antioxidants on the activated leukocytes-induced mutagenesis in the co-culture assay systems. Biosci Biotechnol Biochem. 2004; 68(1):238–242. [PubMed: 14745192]
26. Sheh A, Lee C-W, Masamura K, Rickman BH, Nohmi T, Wogan GN, Fox JG, Schauer DB. Mutagenic potency of *Helicobacter pylori* in the gastric mucosa of mice is determined by gender and duration of infection. Proc. Nat. Acad. Sci. USA. 2010; 107:15217–1522. [PubMed: 20699385]
27. Levy JA, Virolainen M, et al. Human lymphoblastoid lines from lymph node and spleen. Cancer. 1968; 22(3):517–524. [PubMed: 5673231]
28. Skopek TR, Liber HL, et al. Isolation of a human lymphoblastoid line heterozygous at the thymidine kinase locus: possibility for a rapid human cell mutation assay. Biochem Biophys Res Commun. 1978; 84(2):411–416. [PubMed: 214074]
29. Li CQ, Robles AI, et al. Apoptotic signaling pathways induced by nitric oxide in human lymphoblastoid cells expressing wild-type or mutant p53. Cancer Res. 2004; 64(9):3022–3029. [PubMed: 15126337]

30. Li CQ, Wright TL, et al. Biological role of glutathione in nitric oxide-induced toxicity in cell culture and animal models. Free Radic Biol Med. 2005; 39(11):1489–1498. [PubMed: 16274884]
31. Richardson KK, Fostel J, et al. Nucleotide sequence of the xanthine guanine phosphoribosyl transferase gene of E. coli. Nucleic Acids Res. 1983; 11(24):8809–8816. [PubMed: 6324102]
32. Chen B, Deen WM. Effect of liquid depth on the synthesis and oxidation of nitric oxide in macrophage cultures. Chem.Res.Toxicol. 2002; 15:490–496. [PubMed: 11952334]
33. Zhuang JC, Wogan GN. Growth and viability of macrophages continuously stimulated to produce nitric oxide. Proc. Natl. Acad. Sci. USA. 1997; 94:11875–11880. [PubMed: 9342330]
34. Hollenbach S, Dhenaut A, Eckert I, Radicella JP, Epe B. Overexpression of Ogg1 in mammalian cells: effects on induced and spontaneous oxidative DNA damage and mutagenesis. Carcinogenesis. 1999; 20:1863–1868. [PubMed: 10469635]
35. Lai CS, Hopwood LE, Hyde JS, Lukiewicz S. ESR studies of O_2 uptake by Chinese hamster ovary cells during the cell cycle. Proc. Natl. Acad. Sci. USA. 1982; 79:1166–1170. [PubMed: 6280170]
36. Nalwaya N, Deen WM. Nitric oxide, oxygen, and superoxide formation and consumption in macrophage cultures. Chem.Res.Toxicol. 2005; 18:486–493. [PubMed: 15777088]
37. Ferguson LR, Turner PM, Hart DW, Tindall KR. Amsacrine-induced mutations in AS52 cells. Environ Mol Mutagen. 1998; 32(1):47–55. [PubMed: 9707098]
38. Li C-Q, Wogan GN. Nitric oxide modulation of apoptosis. Cancer Lett. 2005; 226:1–15. [PubMed: 16004928]
39. Lewis RS, Deen WM. Kinetics of the reaction of nitric oxide with oxygen in aqueous solutions. Chem. Res. Toxicol. 1994; 7:568–574. [PubMed: 7981422]
40. Chen, Bo; Deen, WM. Analysis of the effects of cell spacing and liquid depth on nitric oxide and its oxidation products in cell cultures. Chem.Res.Toxicol. 2001; 21:2134–2147.
41. Weisenberger S, Schumpe A. Estimation of gas solubility in salt solutions at temperatures from 273K to 363K. AIChE J. 1996; 42:298–300.
42. Zacharia I, Deen WM. Diffusivity and solubility of nitric oxide in water and saline. Ann. Biomed. Engr. 2005; 33:214–222.
43. Goldstick TK, Fatt I. Diffusion of oxygen in solutions of blood proteins. Chem. Eng. Prog. Symposium Ser. 99. 1970; 66:101–107.

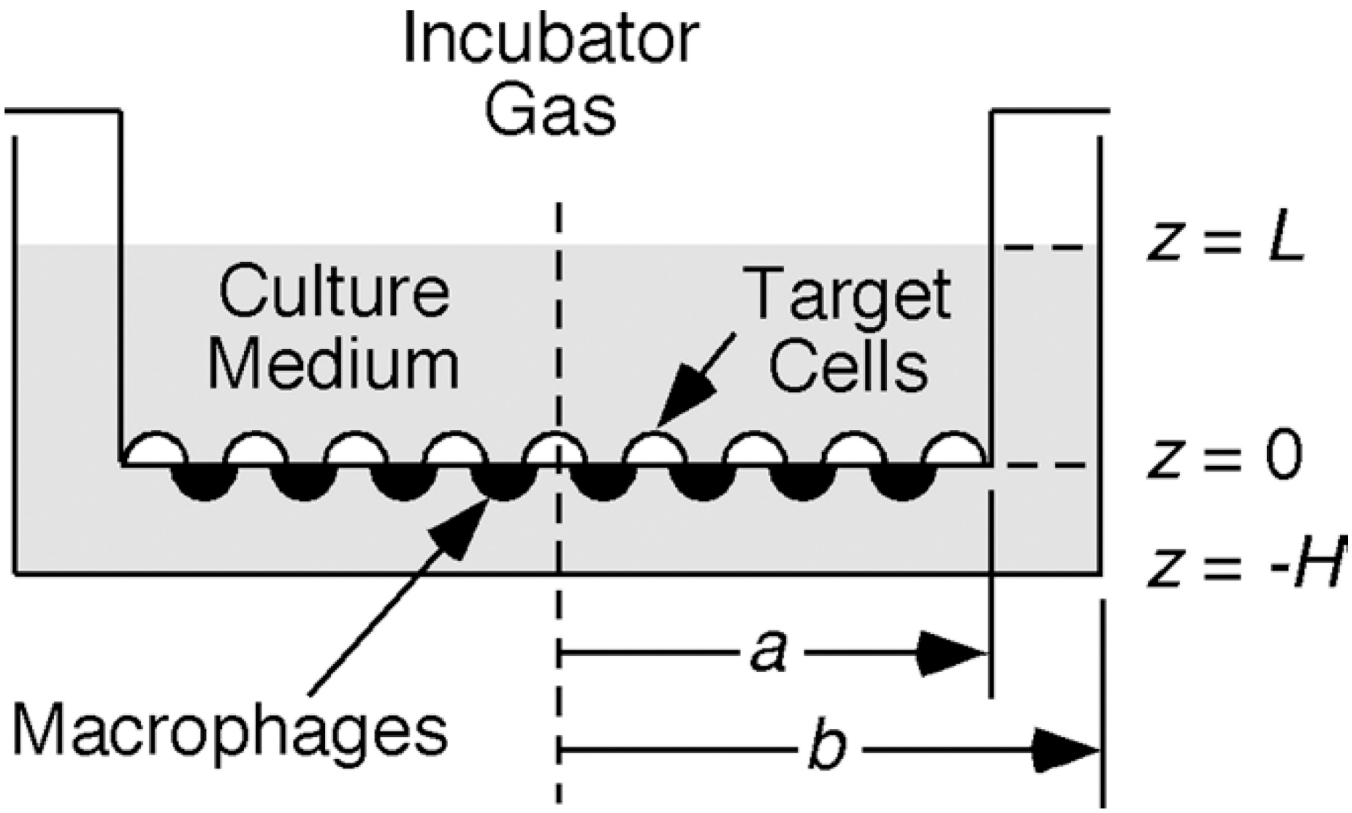

Figure 1.
Schematic of co-culture system. A porous insert of radius *a* fits within an outer dish of radius *b*. Macrophages adhere to the bottom of the insert and target cells are on the top. The positions of the bottom of the dish, membrane with cells, and top of the liquid are $z = -H$, $z = 0$, and $z = L$, respectively.

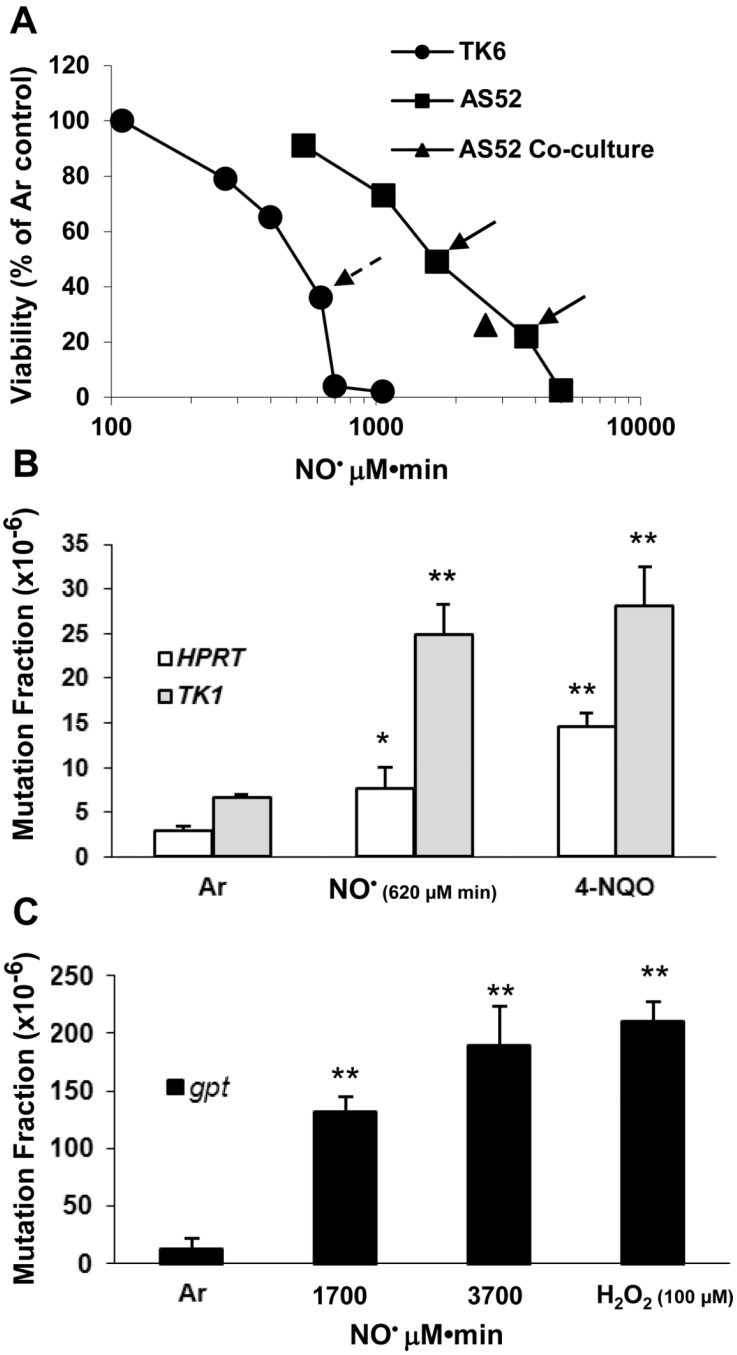

Figure 2.

Cytolethality and mutagenicity of pre-formed NO• in TK6 and AS52 cells. A. Dose-response of loss of viability vs cumulative total dose of NO•. B. Mutagenicity of NO• in *HPRT* and *TK1* genes of TK6 cells. C. Mutagenicity of NO• in gpt gene of AS52 cells.

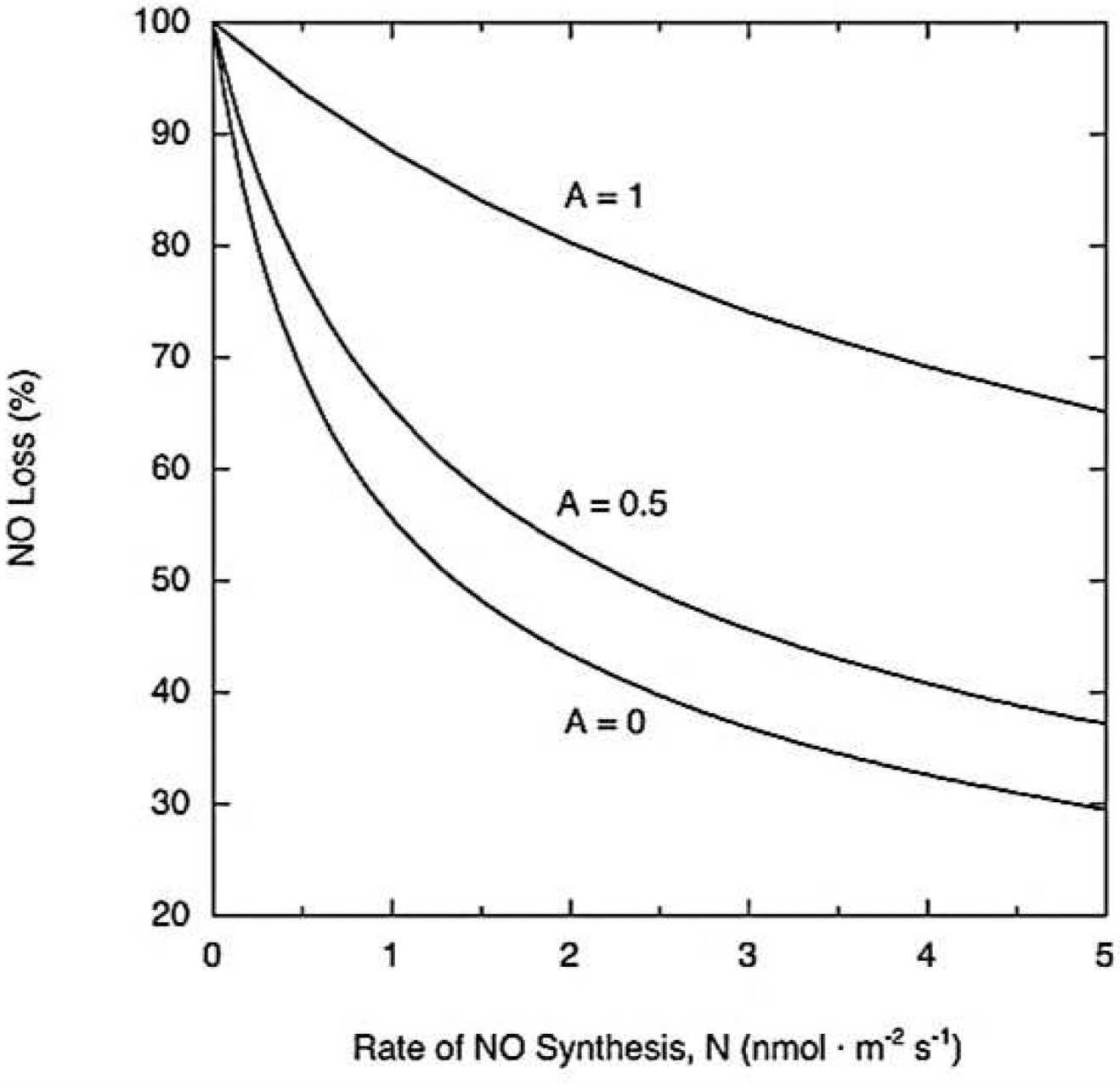

Figure 3.

Effect of the cellular rate of NO• synthesis on its loss from the co-culture system. The predicted percentage of NO• lost by diffusion out of the liquid is shown for three values of the O_2 consumption parameter, ranging from $A = 0$ (negligible O_2 consumption by cells) to $A = 1$ (maximal O_2 consumption).

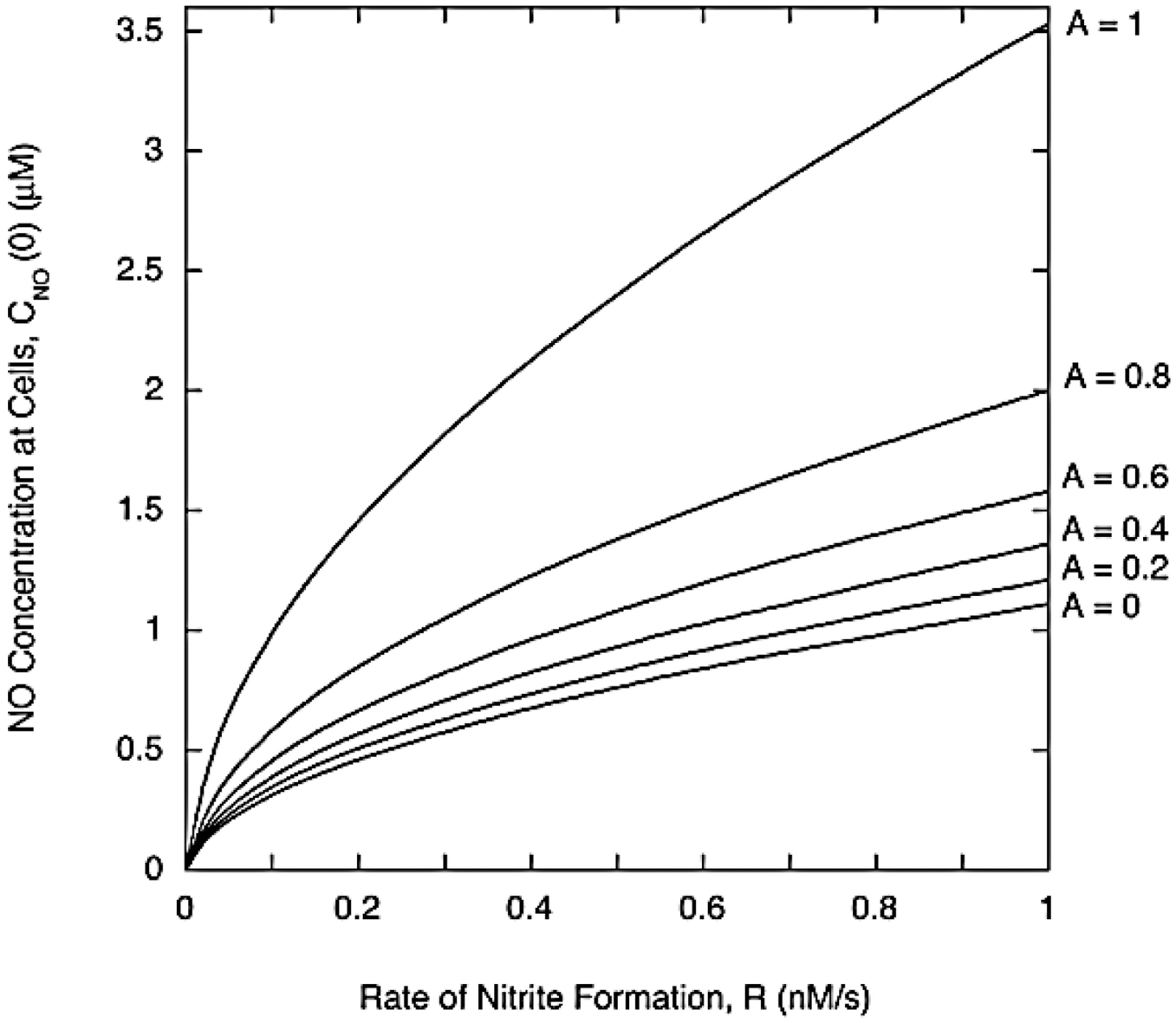

Figure 4.

Cellular concentration of $NO^{\bullet}$ in the co-culture system as a function of the rate of NO_2^- formation. Results are shown for six values of the O_2 consumption parameter, ranging from $A = 0$ (negligible O_2 consumption by cells) to $A = 1$ (maximal O_2 consumption). The use of this plot to estimate $NO^{\bullet}$ concentrations from NO_2^- measurements is described in the text.

Chem Res Toxicol. Author manuscript; available in PMC 2013 April 16.

Table 1

Viability, mutation frequency, and $NO^{\bullet}$ concentration and dose for AS52 cells co-cultured with RAW 264.7 cells.

Conditions	Viability (% Control)	MF ($\times 10^{-6}$)	NO_2^- Conc. (μM)	$NO^{\bullet}$ Conc. (μM)	$NO^{\bullet}$ Dose (μM • min)
Unactivated	100	18 ± 2	45 ± 0.7		
IFN-γ/LPS					
15 h	74 ± 5*	55 ± 12*	-----		
24 h	34 ± 1*	90 ± 13*	-----		
48 h	26 ± 3**	170 ± 18**	127 ± 10**	1.05	2650
48 h + NMA	83 ± 7	50 ± 9*	16 ± 1.3**	0.36	910
48 h + NMA +Tiron	94 ± 6	27 ± 3	13 ± 0.5**	0.32	810
48 h + NMA +Tiron +Uric acid	94 ± 5	26 ± 5	14 ± 0.6**	0.33	830

* $p < 0.05$

** $p < 0.01$ as compared to co-culture with unactivated macrophages.

MF is mutation frequency.

TABLE 2

PCR Analysis of *gpt* in mutant AS52 Cells after NO• Exposure by Reactor and Co-culture Systems

	Number of mutants (%)			
	Reactor		Co-culture	
	Spontaneous[a]	NO•-induced[b]	Spontaneous[c]	NO•-induced[d]
No change in PCR amplimer size[e]	15 (79)	30 (61)	17 (77)	30 (60)
Large deletions/rearrangements[f]	4 (21)	19 (39)	5 (23)	21 (40)
Total of mutants analyzed	**19 (100)**	**49 (100)**	**22 (100)**	**51 (100)**

[a] Cells exposed to argon gas under the same conditions served as negative controls.

[b] Cells exposed to 2520 μM min of NO•.

[c] Untreated cells served as negative control.

[d] Cells co-cultivated with IFN-γ/LPS-stimulated RAW264.7 cells for 48 h.

[e] No changes were observed after PCR reactions.

[f] Large deletions or rearrangements resulting in the absence of PCR amplified *gpt* sequences [Complete deletions (0.5 + 0.8 kb) and deletions of the 0.5 kb with normal 0.8 kb product].

TABLE 3

Summary of the *gpt* Mutation Spectra in AS52 Cells after NO• Exposure by Reactor and Co-culture Systems

	Number of mutants (%)			
	Reactor		Co-culture	
	Spontaneous[a]	NO•-induced[b]	Spontaneous[c]	NO•-induced[d]
Transversion	6 (40)	14 (46)	5 (29)	13 (43)
G:C to T:A	5 (33)	10 (33)	5 (29)	10 (33)
G:C to C:G	1 (7)	0 (0)	0 (0)	1 (3)
A:T to T:A	0 (0)	1 (3)	0 (0)	2 (7)
A:T to C:G	0 (0)	3 (10)	0 (0)	0 (0)
Transition	1 (7)	3 (10)	1 (6)	7 (23)
G:C to A:T	1 (7)	3 (10)	1 (6)	6 (20)
A:T to G:C	0 (0)	0 (0)	0 (0)	1 (3)
Insertions	1 (7)	2 (7)	1 (6)	2 (7)
Deletions	7 (46)	11 (37)	9 (53)	6 (20)
Multiple	0 (0)	0 (0)	1 (6)	2 (7)
Total	**15 (100)**	**30 (100)**	**17 (100)**	**30 (100)**

[a]Cells exposed to argon gas under the same conditions served as negative controls.

[a]Cells exposed to 2520 μM min of NO•.

[c]Untreated cells served as negative control.

[d]Cells co-cultivated with IFN-γ/LPS-stimulated RAW264.7 cells for 48 h.